Defect-Induced (Dis)Order in Relaxor Ferroelectric Thin Films

Sahar Saremi,[1] Jieun Kim,[1] Anirban Ghosh,[1] Derek Meyers,[1] and Lane W. Martin[1,2,*]
[1]*Department of Materials Science and Engineering, University of California, Berkeley, Berkeley, California 94720, USA*
[2]*Materials Sciences Division, Lawrence Berkeley National Laboratory, Berkeley, California 94720, USA*

The effect of *intrinsic* point defects on relaxor properties of 0.68 $PbMg_{1/3}Nb_{2/3}O_3$-0.32 $PbTiO_3$ thin films is studied across nearly 2 orders of magnitude of defect concentration via *ex post facto* ion bombardment. A weakening of the relaxor character is observed with increasing concentration of bombardment-induced point defects, which is hypothesized to be related to strong interactions between defect dipoles and the polarization. Although more defects and structural disorder are introduced in the system as a result of ion bombardment, the special type of defects that are likely to form in these polar materials (i.e., defect dipoles) can stabilize the direction of polarization against thermal fluctuations, and in turn, weaken relaxor behavior.

Relaxor ferroelectrics are characterized by a broad maximum in temperature-dependent dielectric permittivity, a strong frequency dispersion of dielectric response below the temperature of maximum permittivity (T_{max}), and the absence of long-range ferroelectric order at zero field [1,2]. Relaxors also exhibit high dielectric permittivity over a broad temperature range, large electromechanical response, and negligible hysteresis [1–3]. Owing to these unique properties, relaxors have been used in a wide range of applications. Common to all relaxors, and strongly influencing their properties, is the existence of some degree of disorder in their crystalline structure [2,4]. Point defects, therefore, can be a valuable tool for controlling relaxor behavior, since they can create both random electric and strain fields [4]. In complex oxides, for example, *extrinsic* substitutional defects (i.e., dopants) have been extensively used to introduce compositional disorder and to manipulate relaxor behavior (i.e., to induce, strengthen, or weaken the relaxor character) [4–7]. The role of *intrinsic* point defects (i.e., vacancies, interstitials, and substitutional defects related to the constituent elements, their complexes and clusters), on the other hand, is less developed. Structural disorder induced by intrinsic point defects can induce relaxor character in nonrelaxors as in strontium-deficient $SrTiO_3$ [8], lanthanum-substituted $PbTiO_3$ where the resulting cation vacancies can weaken long-range order and induce relaxor character [9], and in lead scandium tantalate and lead scandium niobate wherein intrinsic vacancies can affect the degree of cation ordering and relaxor character [10,11]. A full understanding of how various types and concentrations of intrinsic point defects affect the properties of relaxor ferroelectrics, however, is lacking.

This paucity of knowledge regarding the role of intrinsic point defects is primarily related to difficulties in on-demand and controlled production of such defects, which are typically formed during the synthesis process with their concentration and type being dictated by the laws of thermodynamics [12]. Recent studies on complex-oxide thin films have, however, shown that energetic ion beams are effective for *ex post facto* production of intrinsic point defects with control over their type, concentration, and location [13–20]. This controlled defect production provides opportunities for the systematic study of defect-property relations in relaxors. Here, although the introduction of point defects is shown to increase the structural disorder, strong interactions between specific defect types that are likely to form in these polar materials (i.e., defect dipoles) and polarization is hypothesized to be responsible for the suppression of the polarization fluctuations and weakening of the relaxor behavior. Ultimately, having the ability to carefully control both concentration and type of point defects is necessary in controlling and understanding relaxor materials physics.

We have investigated the effect of bombardment-induced intrinsic point defects on the relaxor behavior of pulsed-laser deposited, 55 nm 0.68 $PbMg_{1/3}Nb_{2/3}O_3$-0.32 $PbTiO_3$ (PMN-PT)/25 nm $Ba_{0.5}Sr_{0.5}RuO_3/NdScO_3$ (110) thin-film heterostructures, across nearly 2 orders of magnitude of defect concentrations (see Supplemental Material for details [21]). A 3.04 MeV helium-ion beam is used for defect production, and the concentration of the induced defects is controlled by the ion dose (3.33×10^{14}–10^{16} ions cm^{-2}). Stopping and range of ions in matter (SRIM) simulations [22] show that intrinsic vacancies, including oxygen (~42%), lead (~32%), niobium (~13%), titanium (~8%), and magnesium (~5%) vacancies, are formed with uniform concentrations across the thickness of the PMN-PT layer as a result of collision events between the incoming helium ions and

target atoms (Supplemental Material, Fig. S1(a) [21]). The total initial concentration of induced defects is calculated to vary from $\sim 10^{18}$ to $\sim 10^{20}$ cm^{-3}, for the ion-dose range used. It is important to note that the helium ions are implanted at a depth of ~ 14.5 μm within the $NdScO_3$ substrate (Supplemental Material, Fig. S1(b) [21]); therefore, the concentration of helium ions in the relaxor is effectively zero, and the observed defect-induced effects can be primarily attributed to the induced intrinsic defects.

Formation of structural defects in the bombarded heterostructures is confirmed by x-ray diffraction studies (Supplemental Material, Fig. S2 [21]). $\theta - 2\theta$ x-ray diffraction studies reveal that the heterostructures are fully epitaxial and single phase for all doses (Supplemental Material, Fig. S2(a) [21]). An enlargement of the $\theta - 2\theta$ scans about the 002- and 220-diffraction conditions, however, reveals a systematic out-of-plane lattice expansion with increasing dose (Supplemental Material, Fig. S2(b) [21]) which is attributed to the formation of point defects such as vacancies in many related complex oxides [23,24]. Moreover, although insignificant at doses below 10^{15} ion cm^{-2}, dramatic changes in the crystalline quality are observed at higher doses. This is manifested by broadening of the diffraction peaks, disappearance of the Laue fringes (Supplemental Material, Fig. S2(b) [21]) which occur only in highly crystalline and homogeneous films, and an increase of the full-width-at-half-maximum of the PMN-PT rocking curves as shown in comparison to that of the substrate (Supplemental Material, Fig. S2(c) [21]). We note that similar bombardment-induced changes in the crystallinity of the bottom electrode are expected as the SRIM simulations suggest that the helium ions travel through the bottom electrode. Such changes, however, cannot be directly observed in this case, due to overlap of the electrode and substrate x-ray peaks, but are expected to have a minimal effect on the properties observed herein. These observations point to increased structural disorder in the system with increasing ion dose as a result of the formation of bombardment-induced point defects. In turn, these materials, provide the opportunity to study the effect of point defects on the evolution of relaxor behavior across nearly 2 orders of magnitude of defect concentration and at varying degrees of disorder.

To study the impact of the induced defects on the relaxor behavior, we probed the evolution of the dielectric response as a function of ion dose (see Supplemental Material for details [21], which includes Ref. [25]). Dielectric permittivity studies as a function of frequency [Fig. 1(a)] reveal a number of changes. First, a dose-dependent reduction in dielectric permittivity and loss is observed, consistent with effects attributed to the presence of defects in similar systems [26–28]. A systematic reduction in frequency dispersion is also observed with increasing bombardment and is almost fully suppressed in highly bombarded heterostructures [Figs. 1(a) and 1(b)]. To better understand these changes, temperature-dependent studies were also

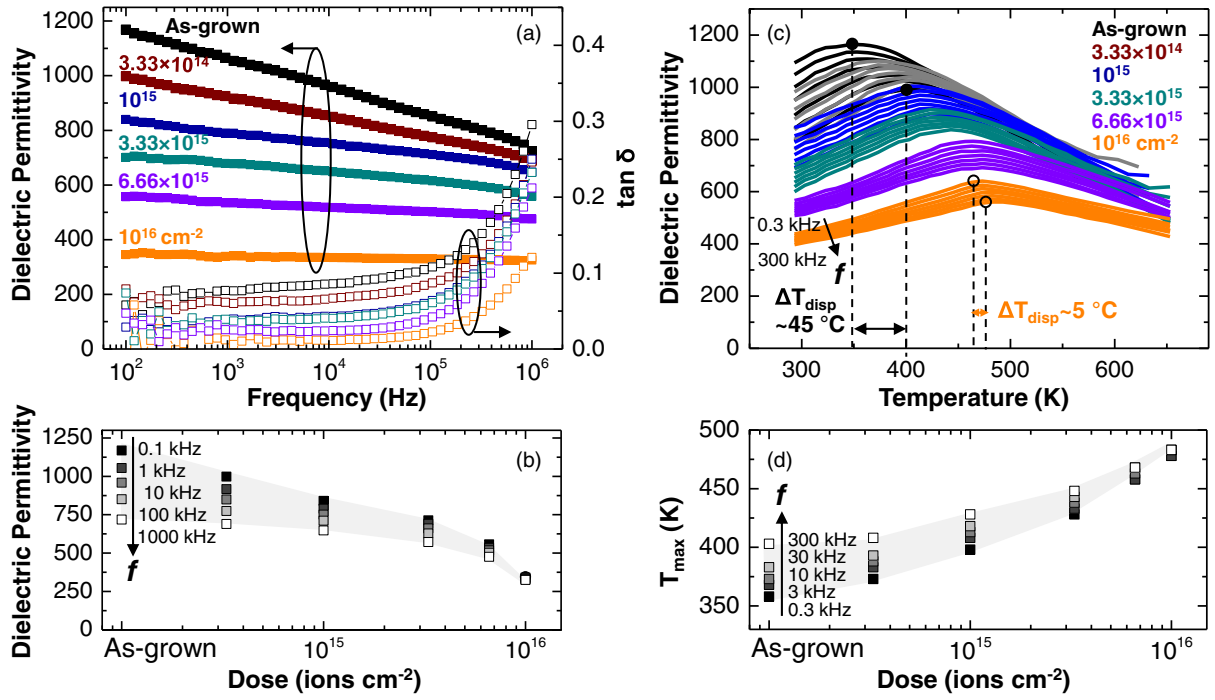

FIG. 1. (a) Room-temperature dielectric permittivity (filled squares) and loss (open squares) as a function of frequency for heterostructures bombarded with various ion doses. (b) Dielectric permittivity as a function of ion dose extracted at various frequencies (0.1–1000 kHz). (c) Dielectric permittivity as a function of temperature and frequency (0.3–300 kHz) for heterostructures bombarded with various ion doses. (d) Extracted values of T_{max} as a function of ion dose at various frequencies (0.3–300 kHz).

completed [Fig. 1(c)]. While a frequency-dependent change in the dielectric maximum temperature ($\Delta T_{disp} = T_{max}^{300\ kHz} - T_{max}^{0.3\ kHz}$; which characterizes the strength of the relaxor behavior [29]) and strong frequency dispersion below T_{max} (as expected for relaxor ferroelectrics) can be observed in the as-grown heterostructures ($\Delta T_{disp} \approx 45$ K), the frequency dependence of the response systematically weakens as the ion dose is increased [Fig. 1(d)]. For example, the heterostructures exposed to 10^{16} ion cm^{-2} show negligible dispersion ($\Delta T_{disp} < 5$ K). It is also important to note that, in addition to a suppression of the frequency dispersion, T_{max} shifts to higher temperatures with increasing dose [Figs. 1(c) and 1(d)]. These observations suggest a weakening of the relaxor character as a result of increasing defect concentration. Thus, we note that the increased structural disorder (due to the displacement of the atoms from their ideal lattice sites) is not the only factor affecting the relaxor response.

A similar increase of T_{max} and decrease of ΔT_{disp} has been previously reported as a result of compressive strain in relaxor thin films [30–32], and has been related to changes of the correlation length and polar nanoregion morphology, and the direction of dipoles within them [30–34]. To examine whether defect-induced changes in the morphology of the local-polar order are responsible for the weakening of the relaxor response, a series of two-dimensional reciprocal space mapping studies was conducted (Supplemental Material, Figs. S3(a)–S3(e) [21]). Two-dimensional KL cuts about the PMN-PT 002-diffraction condition reveal classic butterfly shaped diffuse-scattering patterns, with diffuse rods extending along the [011] and $[0\bar{1}1]$ for all doses. Although increased peak broadening and lattice expansion can be observed in both the film and substrate diffraction peaks with increasing dose, the overall shape of the diffuse-scattering patterns remains unchanged. Intensity profiles along the [011] are also extracted (Supplemental Material, Fig. S3(f) [21]), and show no significant changes as a function of dose. These observations imply that there is no change in the shape or size of the polar nanoregions as a result of the introduction of defects and, thus, additional considerations are required to explain the dose-dependent evolution of the relaxor behavior.

To further explore the origin of the defect-induced effects, polarization-electric field hysteresis loops were measured at a frequency of 10 kHz as a function of temperature and ion dose [Figs. 2(a)–2(f)], and the width of the hysteresis loops at zero polarization, and shift of the center of the hysteresis loops on the field axis were extracted [Figs. 2(g)–2(i)]. The as-grown heterostructures show slim hysteresis loops at room temperature (typical of relaxor ferroelectrics) [Fig. 2(a)]. Upon reducing the temperature, however, the width of the hysteresis loops increases from ~40 kV cm^{-1} at room temperature to

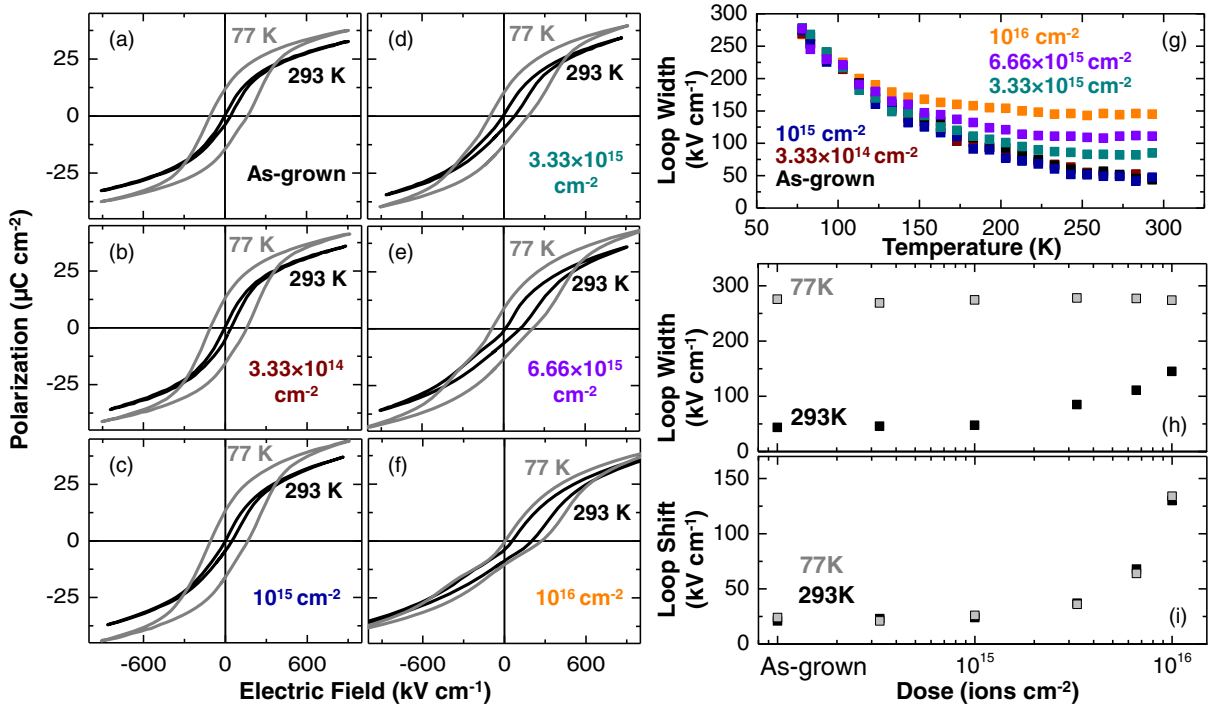

FIG. 2. (a)–(f) Polarization-electric field hysteresis loops measured at a frequency of 10 kHz at 77 K and 293 K for heterostructures bombarded with various ion doses. (g) Width of the hysteresis loops extracted as a function of temperature for heterostructures bombarded with various ion doses. (h) Width of the hysteresis loops as a function of ion dose extracted at 77 and 293 K. (i) Horizontal shift of the hysteresis loops as a function of ion dose extracted at 77 and 293 K.

$\sim$280 kV cm^{-1} at 77 K. Neither the overall shape of the loops [Figs. 2(a)–2(c)] nor the width and shift of the hysteresis loops, at both room temperature and 77 K [Figs. 2(g)–2(i)], exhibit any appreciable changes up to ion does of 10^{15} ions cm^{-2}. At higher doses, however, a number of changes are apparent. A slight pinching appears in the hysteresis loops and becomes more pronounced as the ion dose is increased [Figs. 2(d)–2(f)]. Additionally, a dose-dependent increase in the width of the hysteresis loops is observed at higher temperatures [Figs. 2(g)–2(h)]. At room temperature, for example, the width of the hysteresis loops increase from $\sim$40 to $\sim$160 kV cm^{-1} with increasing dose, but this is less pronounced at lower temperatures (at 77 K, for example, the width of the loops remains constant at $\sim$280 kV cm^{-1}). An increase in the shift of the hysteresis loops is also observed at all temperatures [Fig. 2(i)], from $\sim$24 to $\sim$135 kV cm^{-1}, with increasing dose.

The pinching and horizontal shift of the hysteresis loops are signatures of the formation of defect dipoles (i.e., defect complexes composed of point defects of opposite charge) in the relaxor, similar to effects seen in other polar systems [35,36], and consistent with the evolution of bombardment-induced defects. It is known that as the defect concentration increases, the initially formed point defects can cluster into complexes. Thus, by increasing the ion dose, the concentration of isolated point defects decreases while the concentration of defect complexes increases, causing more pronounced pinching and shifting of the hysteresis loops. Strong interactions between the electric dipole of such defect complexes and the polarization have been predicted and measured [37–40]. Defect dipoles typically align in the direction of the polarization and act as pinning centers for polarization switching, with pinning strengths considerably larger than that of isolated point defects [20,40]. The likely presence of such defect-dipole-polarization coupling could explain the increase of the width of the hysteresis loops at high-ion doses ($>10^{15}$ ions cm^{-2}) where a considerable concentration of defect complexes appears to exist (as indicated by the pronounced shift and pinching of the hysteresis loops). Polarization reversal, on the other hand, is a thermally activated process and the activation-energy barrier for switching increases as the temperature is lowered. As a result, at high temperatures, where thermal fluctuations play a significant role, the pinning effect of defects on polarization reversal is more pronounced as compared to lower temperatures, where the polarization switching is predominantly field driven. Therefore, different ion-dose and temperature regimes can be identified. In the low-dose regime ($<10^{15}$ ions cm^{-2}), where the presence of isolated point defects is more likely, there is no significant change in the switching. Within the high-dose regime ($>10^{15}$ ions cm^{-2}), where defect dipoles are more likely to form, strong defect-polarization interactions (i.e., pinching and an increase of the width and shift of the hysteresis loops) are observed. Within this regime, the effect of defects on polarization reversal is temperature dependent. At high temperatures, the process is limited by the presence of defects (i.e., pinning of polarization by defects), while at low temperatures it is limited by the freezing of polarization fluctuations. This is useful in explaining the evolution of the dielectric response and weakening of the relaxor behavior with increasing ion dose. Based on these observations, it is hypothesized that although more displacement defects (and disorder) are introduced in the system, the special type of defects (i.e., defect dipoles) that are likely to form as the defect concentration is increased, and their ordering, stabilize the direction of the polarization against thermal fluctuations, and, in turn, weaken the relaxor behavior, while the morphology and size of the local-polar order remains effectively unaltered. We also note that our conclusions regarding defect-dipole formation is primarily based on the observed bombardment-induced changes in the hysteresis loops, and that future studies would be worthwhile in further supporting this hypothesis.

To further analyze this defect-induced deviation from relaxor behavior, we have extracted the critical exponent γ (which describes the diffuseness of the phase transition) according to a modified Curie-Weiss law relating the dielectric permittivity ε with temperature T as in

$$\frac{1}{\varepsilon} - \frac{1}{\varepsilon_{\max}} = C^{-1}(T - T_{\max})^{\gamma}, \tag{1}$$

where $\varepsilon_{\max}$ corresponds to the maximum dielectric permittivity and C is a constant [41]. While the dielectric permittivity of a normal ferroelectric follows the Curie-Weiss law above the Curie temperature, relaxors exhibit a temperature dependence of dielectric permittivity that deviates from Curie-Weiss behavior over a wide temperature range above $T_{\max}$. This deviation can be used to characterize the strength of the relaxor behavior and is quantified by the critical exponent γ. For a normal ferroelectric (i.e., sharp transition) $\gamma = 1$, while for an ideal relaxor (i.e., completely diffuse phase transition) $\gamma = 2$ [41–43]. For relaxors, it is not uncommon to find $1 < \gamma < 2$ depending on the strength of the relaxor character [41]. γ was determined for the heterostructures exposed to various doses from the slope of the plot of $\log[(1/\varepsilon) - (1/\varepsilon_{\max})]$ vs. $\log(T - T_{\max})$ [Fig. 3(a)]. For the as-grown heterostructures, $\gamma = 1.82$ which is indicative of strong relaxor character, and there is little change in γ up to a dose of 10^{15} ions cm^{-2}. At higher doses, γ systematically decreases with increasing dose and reaches $\gamma = 1.3$ for a dose of 10^{16} ions cm^{-2}. This reduction of γ above 10^{15} ions cm^{-2} correlates well with the onset of pinching and the dose-dependent increase of the width and shift of the hysteresis loops, and further supports the hypothesis that the formation and ordering of defect dipoles is responsible for the suppression of polarization fluctuations, thus weakening the relaxor behavior.

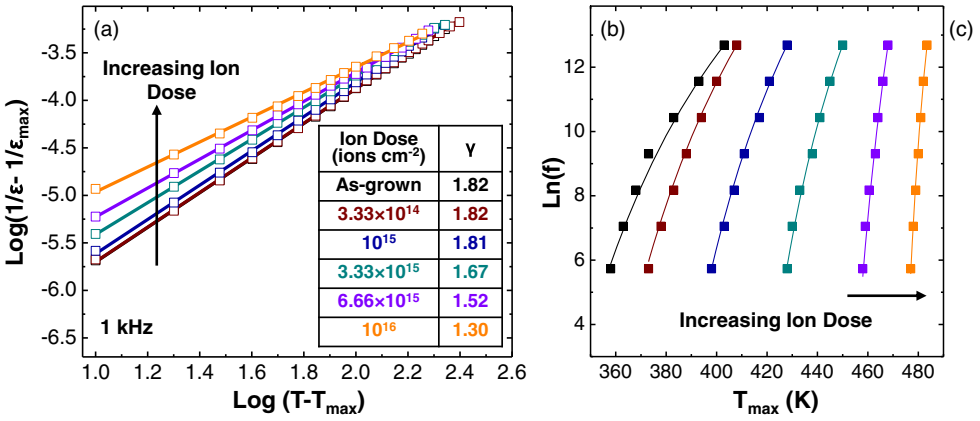

FIG. 3. (a) Plot of modified Curie-Weiss law $\{\log[(1/\varepsilon) - (1/\varepsilon_{\max})]$ vs $\log(T - T_{\max})\}$ for heterostructures bombarded with various ion doses. The critical exponent γ is extracted from the slope of the linear fits (inset). (b) Vogel-Fulcher plot $[\ln(f)$ vs $T_{\max}]$ for heterostructures bombarded with various ion doses. Solid squares and lines correspond to experimental data and fittings, respectively. (c) Vogel-Fulcher parameters extracted from fits of the experimental data for various ion doses.

In addition to deviation of the dielectric response from Curie-Weiss behavior, it is known that, due to the presence of dipolar correlations, the frequency dependence of $T_{\max}$ in relaxors deviates from the Arrhenius dependence expected for normal dielectrics [44,45]. It is generally observed that this dependence obeys an empirical Vogel-Fulcher relation which can be used to study cooperative thermal relaxation processes:

$$f = f_0 \exp\left(\frac{-E_a}{K_B(T_{\max} - T_F)}\right), \qquad (2)$$

where f is the applied ac field frequency, f_0 is the limiting response frequency of the dipoles, E_a is the activation energy, T_F is the static freezing temperature, and K_B is the Boltzmann's constant [44,45]. Vogel-Fulcher fits are obtained from the temperature-dependent dielectric permittivity data [Fig. 3(b)]. The degree of relaxor behavior is represented by the curvature of the $\ln(f)$ vs $T_{\max}$ plot, and is found to reduce with increasing dose as noted by the decreased $T_{\max}$ range and more linear and vertical Vogel-Fulcher curves. Values of T_F, E_a, and f_0 are extracted from the fits of the experimental data [Fig. 3(c)]. While f_0 values are similar and within a reasonable range for thermally activated polarization fluctuations (10^{11}–10^{13} Hz) [44,45] at all doses, there is a systematic reduction of E_a and increase of T_F as the dose is increased. E_a is related to the energy required for a thermally activated and cooperative transition between different polarization configurations and is, therefore, the product of the number of dipoles which are free to take part in the cooperative rearrangement and the chemical potential change associated with the reconfiguration [46]. The reduction of E_a with increasing defect concentration is, thus, consistent with the hypothesis that ordering of special defect types (i.e., defect dipoles) can stabilize the polarization direction, and therefore, reduce the number of lattice dipoles that are free to fluctuate. This is also consistent with the dose-dependent increase of T_F which suggests that the suppression of polarization fluctuations occurs at higher temperatures as the ion dose increases. These observations further confirm the hypothesis that ordering of defect dipoles plays an important role in weakening the relaxor behavior.

In summary, this work demonstrates a weakening of the relaxor character as a result of the formation of intrinsic point defects in PMN-PT thin films, despite a defect-induced increase of structural disorder. Formation and ordering of the defect dipoles are hypothesized to be responsible for observed changes in macroscopic properties. Such ordered defects can stabilize the direction of polarization against thermal fluctuations, and, in turn, weaken the relaxor behavior. This study, therefore, shows the complex effect of point defects in controlling the local (dis)order, and suggests that having the ability to carefully control both the concentration and type of point defects is instrumental in engineering relaxor materials.

S. S. acknowledges support from the U.S. Department of Energy, Office of Science, Office of Basic Energy Sciences, under Award No. DE-SC-0012375 and under the Materials Sciences and Engineering Division under Contract No. DE-AC02-05-CH11231 (Materials Project program KC23MP) for the development of novel ferroic thin-film materials. J. K. acknowledges support from the National Science Foundation under Grant No. DMR-1708615. A. G. acknowledges support from the Army Research Laboratory under Grant No. W911NF-14-1-0104. D. M. acknowledges support from the Gordon and Betty Moore Foundation's EPiQS Initiative, under Grant No. GBMF5307. L. W. M acknowledges support from Intel, Corp. as part of the FEINMAN program.

*Corresponding author.
lwmartin@berkeley.edu

[1] T. R. Shrout and J. Fielding, Jr., in *Proceedings of the IEEE Ultrasonic Symposium* (IEEE, Piscataway, NJ, 1990), Vol. 2, pp. 711–720.
[2] L. E. Cross, Ferroelectrics **151**, 305 (1994).
[3] S.-E. Park and T. R. Shrout, J. Appl. Phys. **82**, 1804 (1997).
[4] F. Chu, I. M. Reaney, and N. Setter, J. Appl. Phys. **77**, 1671 (1995).
[5] M. P. Harmer, J. Chen, P. Peng, H. M. Chan, and D. M. Smyth, Ferroelectrics **97**, 263 (1989).
[6] G. A. Samara, J. Phys. Condens. Matter **15**, R367 (2003).
[7] A. A. Bokov and Z.-G. Ye, J. Mater. Sci. **41**, 31 (2006).
[8] H. W. Jang, A. Kumar, S. Denev, M. D. Biegalski, P. Maksymovych, C. W. Bark, C. T. Nelson, C. M. Folkman, S. H. Baek, N. Balke, C. M. Brooks, D. A. Tenne, D. G. Schlom, L. Q. Chen, X. Q. Pan, S. V. Kalinin, V. Gopalan, and C. B. Eom, Phys. Rev. Lett. **104**, 197601 (2010).
[9] T.-Y. Kim and H. M. Jang, Appl. Phys. Lett. **77**, 3824 (2000).
[10] F. Chu, N. Setter, and A. K. Tagantsev, J. Appl. Phys. **74**, 5129 (1993).
[11] C. Malibert, B. Dkhil, J. M. Kiat, D. Durand, J. F. Berar, and A. Spasojevic-de Bire, J. Phys. Condens. Matter **9**, 7485 (1997).
[12] S. Saremi, R. Gao, A. Dasgupta, and L. W. Martin, Am. Ceram. Soc. Bull. **97**, 16 (2018).
[13] S. B. Krupanidhi, H. Hu, and V. Kumar, J. Appl. Phys. **71**, 376 (1992).
[14] H. Hu and S. B. Krupanidhi, Appl. Phys. Lett. **61**, 1246 (1992).
[15] L. R. Zheng, P. X. Yang, L. W. Wang, C. L. Lin, and S. C. Zo, Nucl. Instrum. Methods Phys. Res., Sect. B **127**, 621 (1997).
[16] S. Mathew, A. Annadi, T. K. Chan, T. C. Asmara, D. Zhan, X. R. Wang, S. Azimi, Z. Shen, A. Rusydi, M. B. Breese, and T. Venkatesan, ACS Nano **7**, 10572 (2013).
[17] S. Saremi, R. Xu, L. R. Dedon, J. A. Mundy, S.-L. Hsu, Z. Chen, A. R. Damodaran, S. P. Chapman, J. T. Evans, and L. W. Martin, Adv. Mater. **28**, 10750 (2016).
[18] L. J. McGilly, C. S. Sandu, L. Feigl, D. Damjanovic, and N. Setter, Adv. Funct. Mater. **27**, 1605196 (2017).
[19] S. Saremi, R. Xu, L. R. Dedon, R. Gao, A. Ghosh, A. Dasgupta, and L. W. Martin, Adv. Mater. Interfaces **5**, 1700991 (2018).
[20] S. Saremi, R. Xu, F. I. Allen, J. Maher, J. C. Agar, R. Gao, P. Hosemann, and L. W. Martin, Phys. Rev. Mater. **2**, 084414 (2018).
[21] See Supplemental Material at http://link.aps.org/supplemental/10.1103/PhysRevLett.123.207602 for additional experimental details and analysis.
[22] J. F. Ziegler, M. D. Ziegler, and J. P. Biersack, Nucl. Instrum. Methods Phys. Res., Sect. B **268**, 1818 (2010).
[23] D. J. Keeble, S. Wicklein, R. Dittmann, L. Ravelli, R. A. Mackie, and W. Egger, Phys. Rev. Lett. **105**, 226102 (2010).
[24] D. Marrocchelli, N. H. Perry, and S. R. Bishop, Phys. Chem. Chem. Phys. **17**, 10028 (2015).
[25] J. C. Frederick, T. H. Kim, W. Maeng, A. A. Brewer, J. P. Podkaminer, W. Saenrang, V. Vaithyanathan, F. Li, L. Q. Chen, D. G. Schlom, and S. Trolier-McKinstry, Appl. Phys. Lett. **108**, 132902 (2016).
[26] F. T. Rogers, Jr., J. Appl. Phys. **27**, 1066 (1956).
[27] L. R. Zheng, P. X. Yang, L. W. Wang, C. L. Lin, and S. C. Zou, Nucl. Instrum. Methods Phys. Res., Sect. B **127**, 621 (1997).
[28] Sun A. Yang, B. H. Kim, M. K. Lee, G. J. Lee, N.-H. Lee, and S. D. Bu, Thin Solid Films **562**, 185 (2014).
[29] I. Grinberg, P. Juhás, P. K. Davies, and A. M. Rappe, Phys. Rev. Lett. **99**, 267603 (2007).
[30] V. Nagarajan, C. S. Ganpule, B. Nagaraj, S. Aggarwal, S. P. Alpay, A. L. Roytburd, E. D. Williams, and R. Ramesh, Appl. Phys. Lett. **75**, 4183 (1999).
[31] V. Nagarajan, S. P. Alpay, C. S. Ganpule, B. K. Nagaraj, S. Aggarwal, E. D. Williams, A. L. Roytburd, and R. Ramesh, Appl. Phys. Lett. **77**, 438 (2000).
[32] P. Miao, Y. Zhao, N. Luo, D. Zhao, A. Chen, Z. Sun, M. Guo, M. Zhu, H. Zhang, and Q. Li, Sci. Rep. **6**, 19965 (2016).
[33] S. Prosandeev, D. Wang, and L. Bellaiche, Phys. Rev. Lett. **111**, 247602 (2013).
[34] J. Kim, H. Takenaka, Y. Qi, A. R. Damodaran, A. Fernandez, R. Gao, M. R. McCarter, S. Saremi, L. Chung, A. M. Rappe, and L. W. Martin, Adv. Mater. **31**, 1901060 (2019).
[35] K. H. H. K. Carl and K. H. Hardtl, Ferroelectrics **17**, 473 (1977).
[36] D. Damjanovic, Rep. Prog. Phys. **61**, 1267 (1998).
[37] U. Robels and G. Arlt, J. Appl. Phys. **73**, 3454 (1993).
[38] W. L. Warren, G. E. Pike, K. Vanheusden, D. Dimos, B. A. Tuttle, and J. Robertson, J. Appl. Phys. **79**, 9250 (1996).
[39] L. Zhang, E. Erdem, X. Ren, and R.-A. Eichel, Appl. Phys. Lett. **93**, 202901 (2008).
[40] A. Chandrasekaran, D. Damjanovic, N. Setter, and N. Marzari, Phys. Rev. B **88**, 214116 (2013).
[41] K. Uchino and S. Nomura, Ferroelectrics **44**, 55 (1982).
[42] H. T. Martirena and J. C. Burfoot, Ferroelectrics **7**, 151 (1974).
[43] X. G. Tang, K.-H. Chew, and H. L. W. Chan, Acta Mater. **52**, 5177 (2004).
[44] D. Viehland, S. J. Jang, L. Eric Cross, and M. Wuttig, J. Appl. Phys. **68**, 2916 (1990).
[45] D. Viehland, M. Wuttig, and L. E. Cross, Ferroelectrics **120**, 71 (1991).
[46] G. Adam and J. H. Gibbs, J. Chem. Phys. **43**, 139 (1965).